Article

Simultaneous Adsorption and Reduction of Cr(VI) to Cr(III) in Aqueous Solution Using Nitrogen-Rich Aminal Linked Porous Organic Polymers

**Muhammad A. Sabri [1], Ziad Sara [2], Mohammad H. Al-Sayah [2], Taleb H. Ibrahim [1], Mustafa I. Khamis [2],*
and Oussama M. El-Kadri [2],***

[1] Department of Chemical Engineering, American University of Sharjah, P.O. Box 26666 Sharjah, UAE;
ashrafsabri87@gmail.com (M.A.S.); italeb@aus.edu (T.H.I.)

[2] Department of Biology, Chemistry, and Environmental Sciences, American University of Sharjah,
P.O. Box 26666 Sharjah, UAE; ziyadsara@gmail.com (Z.S.); malsayah@aus.edu (M.H.A.-S.)

* Correspondence: mkhamis@aus.edu (M.I.K.); oelkadri@aus.edu (O.M.E.-K.)

Abstract: Two novel nitrogen-rich aminal linked porous organic polymers, NRAPOP-O and NRAPOP-S, have been prepared using a single step-one pot Schiff-base condensation reaction of 9,10-bis-(4,6-diamino-S-triazin-2-yl)benzene and 2-furaldehyde or 2-thiophenecarboxaldehyde, respectively. The two polymers show excellent thermal and physiochemical stabilities and possess high porosity with Brunauer–Emmett–Teller (BET) surface areas of 692 and 803 m^2 g^{-1} for NRAPOP-O and NRAPOP-S, respectively. Because of such porosity, attractive chemical and physical properties, and the availability of redox-active sites and physical environment, the NRAPOPs were able to effectively remove Cr(VI) from solution, reduce it to Cr(III), and simultaneously release it into the solution. The efficiency of the adsorption process was assessed under various influencing factors such as pH, contact time, polymer dosage, and initial concentration of Cr(VI). At the optimum conditions, 100% removal of Cr(VI) was achieved, with simultaneous reduction and release of Cr(III) by NRAPOP-O with 80% efficiency. Moreover, the polymers can be easily regenerated by the addition of reducing agents such as hydrazine without significant loss in the detoxication of Cr(VI).

Keywords: porous organic polymers; adsorption; chromium (VI) removal; environmental remediation

1. Introduction

Each year, large amounts of heavy metal ions are released into the aquatic environment from agricultural, industrial and/or natural sources, leading to contamination of water and soil and, thus, presenting a major health risk to humans and animals [1]. Industrial wastewater streams from factories of leather manufacturing, leather tanning, textiles, printing, wood preservation, and electroplating processes are highly contaminated with chromium metal ions [1–3]. The most prevailing and stable forms of chromium in the environment are the trivalent chromium (Cr(III)) and the hexavalent chromium (Cr(VI)) ions [4,5]. The former is a vital micronutrient and relatively water-insoluble at neutral-to-basic pHs and, hence, it presents a low risk for the environment and health [5–7]. However, Cr(VI) is a highly toxic, carcinogenic, non-biodegradable, mutagenic heavy metal, and it could cause reversible renal tubular damage, cardiovascular collapse, and hematological toxicity [6,8–10]. This high toxicity of Cr(VI) is attributed to its high water-solubility, cell-membrane permeability, and strong oxidizing properties. Cr(VI) is speciated in aqueous media in the form of different oxyanions (CrO_4^{2-}, $Cr_2O_7^{2-}$ and $HCrO_4^{-}$) [4,6,11–13].

Environmental agencies worldwide have set the maximum permissible concentration of Cr(VI) in water resources to be as low as 0.05 mg/L [14,15]. This emphasizes the necessity for removal of Cr(VI) ions from industrial wastewater streams before effluent discharge to the aquatic bodies. Accordingly, various chemical and physical processes have

been adopted to ensure the efficient and complete removal of Cr(VI) from effluent streams. Current methods include chemical and electrochemical precipitation, reduction, ion exchange, membrane separation, cementation, reverse osmosis, and adsorption [7,16–24].

The approach to reduce Cr(VI) to Cr(III) offers significant benefits towards Cr(VI) removal from industrial effluent streams [25–28]. The produced Cr(III) from the reduction process has 500–1000 times lower toxicity and mobility than that of Cr(VI); thus, it renders the process environmentally friendly [4,29]. However, this reduction process is energy-intensive from chemical, electrochemical, and photocatalytic perspectives [26,30–32]. Adsorption, on the other hand, has been reported to be a facile, effective and economically feasible method for Cr(VI) removal from aqueous streams [16,19,20,23,24,33]. A number of adsorbents including inorganic substances, agricultural byproducts, biosorbents, activated carbon, carbon based nanomaterials, and porous polymers have been employed for removal of Cr (VI) from aqueous solutions [26,29,34–38]. Recent studies showed the ability of certain adsorbent to reduce Cr(VI) to Cr(III) with simultaneous release of the latter to aqueous media [29,38,39]. However, these adsorbents have limited redox-active sites and/or suffer from irreversible partial oxidation and, hence, impede their application in chromium detoxication. As such, needs still exist for the development of adsorbents possessing large surface areas and abundant redox active sites that are simultaneously able to capture large amounts of Cr(VI), reduce it to Cr(III), and then release the resulting Cr(III) into aqueous medium. Such adsorbents with spontaneous cycles of "capture-reduce-release" of Cr (VI) would allow for efficient detoxication of high concentrations of Cr(VI). An attempt at such a process was reported recently by Ding and coworkers who used a polymer composite (PANI@PS) of polyaniline (PANI) and polystyrene (PS) for simultaneous reduction of Cr(VI) to Cr(III) and the sequestration of Cr(III) from aqueous solutions [29]. However, desorption of Cr (III) from the polymer composite and its regeneration required electrochemical reduction of PANI.

Porous organic polymers (POPs) are a class of porous material that have attracted considerable attention due to their robust nature, high specific surface area, and tunable pore size with diverse functionalities, and, most importantly, possess excellent chemical stability under harsh conditions [40–42]. Because of the many synthetic reaction routes and the availability of a wide range of organic linkers, POPs can be tailored-made for targeted applications. Accordingly, POPs have found applications in gas storage and separation, catalysis, and chemical sensors, among many others [42–46]. Surprisingly, their performance in the removal of Cr(VI) has been limited [47–49].

Recently, we reported a number of aminal linked porous organic polymers (ALPOPs) and their application in small gas molecules and radioactive iodine capture and toxic metal sensing [50–52]. The highly porous ALPOPs are linked by aminal bonds and contain triazine rings, which facilitate their excellent carbon dioxide and iodine uptakes. The presence of amine and imine chemical functionalities in the ALPOPs' frameworks should also provide the desired environment for the chelation of metal ions, adsorption of anionic metal species, and reduction sites [29]. Coupled with such attractive chemical properties are the high surface area and the many redox-active adsorption sites, which make them potential adsorption/reduction materials for Cr (VI). Herein, we present the design and synthesis of two novel nitrogen-rich aminal linked porous organic polymers (NRAPOP-O and NRAPOP-S) by applying metal free, Schiff-base condensation reactions of 9,10-bis-(4,6-diamino-S-triazin-2-yl) benzene and 2-furaldehyde or 2-thiophenecarboxaldehyde, respectively. These novel polymers were further investigated in the simultaneous removal and reduction of Cr (VI) with concurrent release of Cr (III) to solution. While NRAPOP-O is more economical to prepare from readily available material, NRAPOP-S introduces the more electron-rich redox-active sulfur atom into polymer's structure. The results show that these polymers are promising adsorbents for the removal of Cr(VI) contamination from industrial wastewater streams with simultaneous reduction in the feasible contact time.

2. Materials, Methods, and Instrumentations

2.1. Materials

All reagents (2-furaldehyde, 2-thiophenecarboxaldehyde, dimethyl sulfoxide (DMSO), tetrahydrofuran (THF), acetone, methanol, dichloromethane, chloroform, hydrazine hydrate, and sodium chromate) used in this study were obtained from commercial chemical suppliers (Sigma-Aldrich, Acros organics) with the exception of 9,10-bis-(4,6-diamino-S-triazin-2-yl)benzene (BATB), which was prepared according to the procedure in the literature [53]. The chemicals were of analytical grade and used as received without further purification.

2.2. Synthesis of NRAPOPs

2.2.1. NRAPOP-O

To an oven-dried 50-mL round bottom flask, equipped with a magnetic stir bar and condenser, were added BATB (500 mg, 1.69 mmol), 2-furaldehyde (650 mg, 6.76 mmol), and DMSO (20 mL). The suspension was bubbled with argon gas for 20 min, and then heated at 180 °C for three days in an oil bath. After cooling the reaction mixture to room temperature, the precipitate was filtered, washed thoroughly with THF, acetone, methanol, and dichloromethane, and dried under vacuum at 120 °C to produce NRAPOP-O as a black colored powder in 62% yield. Anal. Calcd. for $C_{32}H_{24}N_{10}O_4$: C, 62.74%; H, 3.95%; N, 22.86%; Found C, 49.06%; H, 5.05%; N 22.01%.

2.2.2. NRAPOP-S

In a similar fashion to the preparation of NRAPOP-O, NRAPOP-S was synthesized by mixing BATB (500 mg, 1.69 mmol), thiophene-2-carbaldehyde (760 mg, 6.68 mmol), and DMSO (20 mL) in a 50-mL round bottom flask. The mixture was heated for three days at 180 °C. A yellow colored powder, NRAPOP-S, in 67% yield was obtained after workup. Anal. Calcd. for $C_{32}H_{24}N_{10}S_4$: C, 56.78%; H, 3.57%; N, 20.69%; Found C, 49.41%; H, 5.45%; N 27.40%.

2.3. Adsorption and Reduction of Cr(VI) by NRAPOPs

Cr (VI) adsorption and reduction studies were carried out at batch bench scale to determine the optimum parameters for Cr (VI) treatment using NRAPOPs. Stock Cr(VI) solution of 1000 mg/L was prepared by dissolving 2.83 g of potassium dichromate in distilled water to a total volume of 500 mL. The desired Cr(VI) concentrations were prepared by appropriate dilutions of the stock solution with distilled water. In batch bench scale experiments, pre-weighed amounts of the NRAPOPs were mixed with 5 mL of Cr(VI) solution of known concentration and agitated at pre-determined time intervals. The total chromium (Cr) concentration was determined using an atomic absorption spectrophotometer. The Cr(VI) concentration was determined spectrophotometrically using method 7196A [38]. The amount of Cr(VI) reduced to Cr(III) was determined as a difference between the total chromium and Cr(VI) concentrations in the aqueous solution. Similar adsorption–reduction experiments were carried out at different experimental parameters—NRAPOPs dosage (0.5–12 g/L), contact time (0–12 days), pH (2–5), temperature (25–45 °C), and initial Cr (VI) concentration (0–100 mg/L)—in order to determine the optimum experimental parameters and reduction efficiencies. The pH was adjusted using either 0.1 M HCl or 0.1 NaOH solutions.

2.4. Instrumentations

Elemental analyses were carried out using a EuroEA3000 series CHNS elemental analyzer (Eurovector Instruments). A Bruker-400 MHz NMR spectrometer was used to obtain the ^{1}H NMR spectra for the BATB building block. Fourier transform infrared (FT-IR) spectra, using KBr pellet as the medium, were obtained by the use of a PerkinElmer FT-IR spectrometer. The theromgravimetric analyses (TGA) were conducted under oxygen flow using a Perkin thermo-gravimetric analyzer with a heating ramp of 5 °C/min. The samples

were heated from room temperature to 800 °C. X-ray powder diffraction (PXRD) patterns were collected using a Panalytical X'pert pro multipurpose diffractometer with Cu Kα radiation with a 2θ range of 5–50. A Quantachrome Autosorb iQ volumetric analyzer was used to perform the porosity study of the NARPOPs in which nitrogen gas of ultra-high purity grade was used. The samples (40–50 mg) were degassed by heating at 120 °C under vacuum for 8 h prior to each measurement. The nitrogen adsorption/desorption isotherms were attained at 77 K using a cryo-bath of liquid nitrogen. The obtained isotherms were used to calculate the Brunauer–Emmett–Teller (BET) surface area, pore size distribution and pore volume. A temperature-controlled flask shaker, TH 15-Edmund Buhler, was used for shaking and temperature control. A pH meter (3320, JENWAY Ltd.) was utilized for pH measurements. Total chromium concentration was measured using an atomic absorption spectrometer (SpectraAA 220FS Varian).

3. Results and Discussion

3.1. Synthesis and Characterization

The novel polymers (NRAPOPs) were prepared in high yields through one-pot Schiff base condensation reaction. Treatment of the core amine-based building block, BATB, with four equivalents of the two aldehyde monomers, 2-furaldehyde or thiophene-2-carbaldehyde in DMSO under reflux for three days and inert atmosphere, afforded black (NRAPOP-O) and yellow (NRAPOP-S) colored powders, respectively, as depicted in Scheme 1. The two porous polymers are insoluble in common organic solvents such as acetone, THF, chloroform, etc., or diluted aqueous acids (HCl) or bases (NaOH), hinting to highly cross-linked structures and good chemical stability.
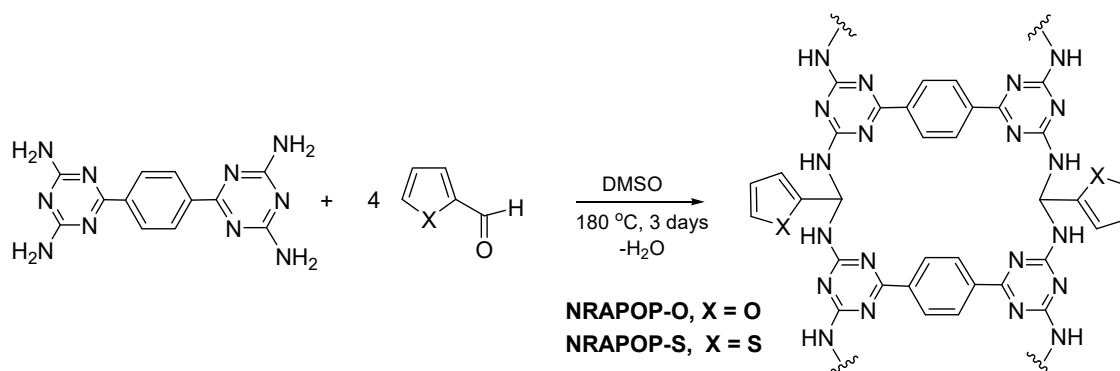
Scheme 1. Preparation of the NRAPOPs.

The chemical connectivity and structure of the polymers' networks were determined by spectroscopic and analytical techniques. The FT-IR spectra (Figure 1A) indicate the formation of aminal bonds (linkages) between the building blocks by the presence of a broad peak at 3415 cm^{-1} assigned to a secondary amine stretching vibration (N-H) and at 2960 and 2915 cm^{-1} due to the methanetriyl (C-H) groups [50,51,54]. In addition, the distinct quadrant stretch at 1542 cm^{-1} provides evidence for the inclusion of the BATB building block in the polymer's networks. Meanwhile, the absence of the C=O stretching at ~1680 cm^{-1} of the two aldehyde monomers (Supplementary Materials, Figure S1) clearly indicates the conversion of the functional groups and the formation of hyper-cross-linked structures. Furthermore, the lack of bands at 1620 cm^{-1} suggests that no imine C=N bond formation occurred and gives further evidence that the monomers are linked by only aminal bonds. Chemical structures for many aminal linked polymers have been confirmed using solid-state ^{13}C NMR technique [51,54–56]. The PXRD spectra (Figure S2) indicate amorphous structures, showing only a single broad diffraction peak. The TGA analysis studies (Figure 1B) indicate the two polymers possess high thermal stability up to 400 °C. The amorphous nature and high thermal stabilities of these NRAPOPs are well documented for many other porous organic polymers with similar network structures [50,51,54–56].
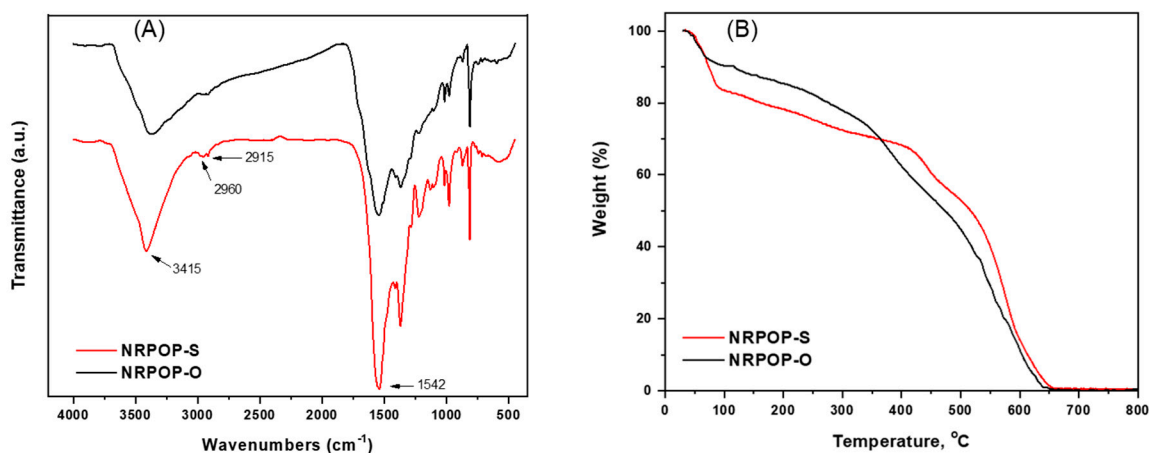
Figure 1. FT-IR spectra (**A**) and TGA curves (**B**) of the NRAPOPs.

3.2. Porosity Study

Pore characteristics and specific surface area of the NRAPOPs were determined through nitrogen adsorption–desorption isotherms (Figure 2A) at 77 K. The BET surface area of NRAPOP-O and NRAPOP-S were recorded to be 692 and 803 m^2 g^{-1} while the total pore volumes were determined to be 1.27 and 1.36 cm^3 g^{-1}, respectively. The type-I nitrogen adsorption–desorption isotherms (Figure 2A) of the NRAPOPs display sharp nitrogen gas uptake at low pressure (P/Po), which reflect their microporous structures [57]. Applying the DFT model, both polymers were found to have similar pore size distribution, mainly at 0.70 and 1.06 nm (Figure 2B).
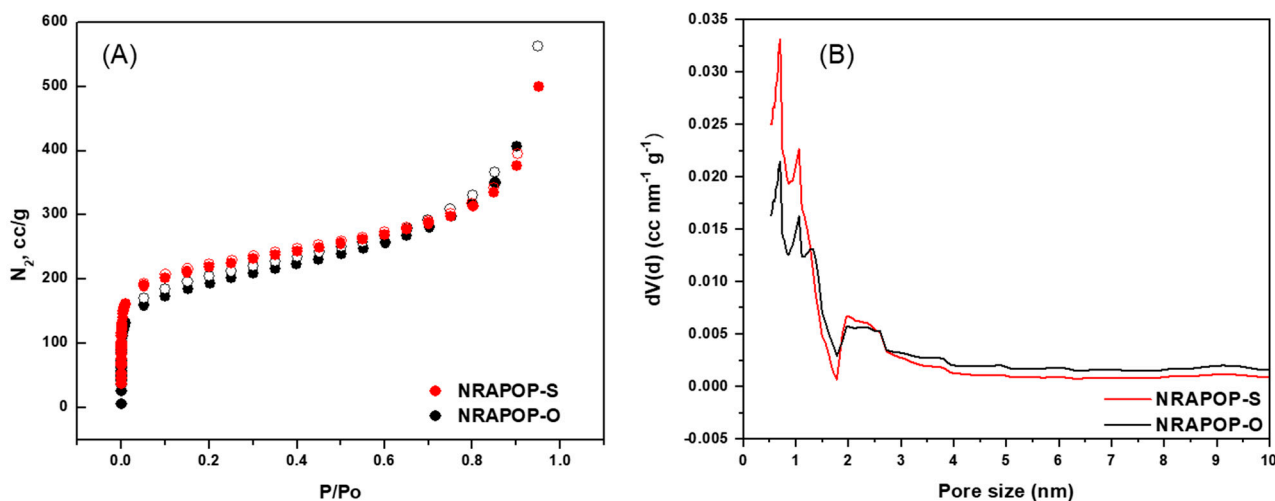

Figure 2. Nitrogen adsorption–desorption isotherms at 77 K (**A**) and pore size distribution (**B**) of the NRAPOPs.
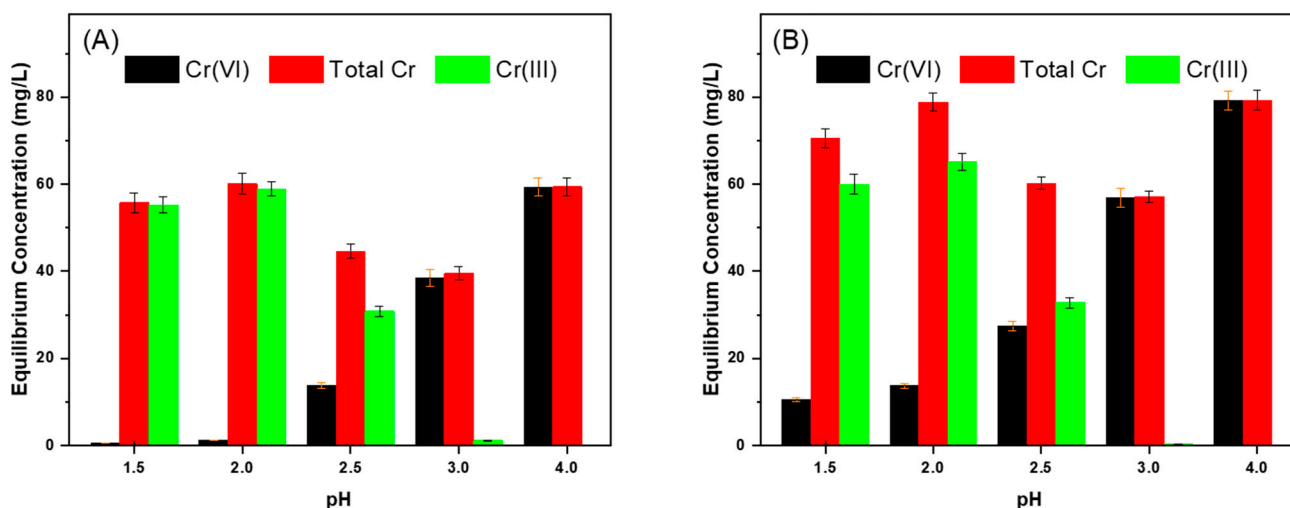
3.3. Adsorption and Reduction of Cr(VI) to Cr(III)

3.3.1. Effect of Initial pH

The chemical speciation of chromium and the adsorption ability of the NRAPOPs are highly impacted by the pH of the solution. In acidic solutions (pH < 5), Cr(III) is soluble and mostly exists as $[Cr(H_2O)_6]^{3+}$ ion, while Cr(VI) exist as $HCrO_4^-$ ion at the pH range of 1.5 to 6 [4–6,11–13]. At neutral-alkaline pHs, Cr (III) is converted to the insoluble Cr (OH)$_3$ while the soluble chromate anion (CrO_4^-) becomes the dominant form of Cr (VI). On the other hand, NRAPOPs' adsorption capacity is also affected by the pH of the solution. At acidic pHs, the polymers are protonated at the nitrogen atoms and this increases the adsorption ability of the material for anions (such as $HCrO_4^-$ and CrO_4^-) and the desorption for cations (such as Cr (III)); the reverse is true at neutral-alkaline

pHs. Therefore, the adsorption ability of the NRAPOPs was evaluated in acidic solution at a pH range of 1.5–4, where Cr (VI) also has a high reduction potential, which makes it more susceptible to reduction. NRAPOPs (8 g/L) were incubated in chromate solutions (100 mg/L) for 24 hrs at different pHs and the concentrations of Cr (VI) and total chromium were measured; the concentration of Cr (III) was then differentially calculated. The results depicted in Figure 3 show that maximum removal of Cr (VI) by NRAPOPs was obtained at pH 1.5–2.0 with almost 100% removal of Cr(VI) from solution (Figure 3A). This is expected at this pH as NRAPOP-O is positively charged (due to protonation), which increases the electrostatic attraction to the Cr(VI) oxyanions ($HCrO_4^-$ and CrO_4^{-2}). However, the concentration of total chromium in solution at this pH range (1.5–2.0) was about 60 mg/L; this indicates that about 40% of the adsorbed metal ion remained attached to the NRAPOP-O while the remaining 60% was reduced to Cr(III) and released to the solution due to the charge similarity. As the pH increased to 4, the concentration of Cr(VI) in solution increased significantly to around 60 mg/L while that of Cr(III) decreased to reach around zero. As for the removal of Cr(VI) by NRAPOP-S, a lower efficiency was observed (Figure 3B). At the pH range from 1.5 to 2.0, a 90% removal of Cr(VI) was achieved, and 66.7% of the adsorbed Cr(VI) was reduced to Cr(III) and released into solution. This indicates that the adsorption capacity of the NRAPOP-S for oxyanions of Cr(VI) decreased due to the decrease in the positive charge of the polymer. At the same pH interval, the reduction to Cr(III) by NRAPOP-S showed a higher efficiency than that observed by NRAPOP-O. This may indicate that the sulfur atom can be more easily oxidized than the oxygen atom on the polymer, which can lead to the observed behavior. As the pH increased to 4, the removal efficiency of Cr(VI) was 20%, which was significantly lower than that observed by NRAPOP-O with no Cr(III) release into solution, which suggests that the NRAPOP-S has lower affinity towards Cr(VI) than that of NRAPOP-O. Such behavior could be attributed to the positive charge density at the two sites of the polymers as a result of the size difference between oxygen and sulfur atoms. However, the observed decease in the reduction of Cr(VI) to Cr(III) as the pH increased is an expected result since the process is known to be catalyzed by the proton [39].

Figure 3. Effect of pH on the adsorption of Cr(VI) and simultaneous reduction of Cr(VI) to Cr(III) using NRAPOP-O (**A**) and NRAPOP-S (**B**). Experimental conditions: dosage: 8 g/L, contact time: 24 h, stirring speed: 175 rpm, temperature: 25 °C, sample volume: 5 mL, initial Cr(VI) concentration: 100 mg/L.

3.3.2. Effect of Dosage

The effect of adsorbent dosage on the adsorption and reduction efficiency of Cr(VI) using the NRAPOPs was studied at the optimal pH of 2 and Cr(VI) concentration of 100 mg/L. The results illustrated in Figure 4 show that the concentration of Cr(VI) in solution decreased as the dosage of NRAPOP-O increased from 1g/L to 8g/L, reaching a 100% removal of Cr(VI) (Figure 4A). Meanwhile, the concentration of Cr(III) in solution increased to become the only species of chromium in solution with a total chromium concentration reaching around 58 mg/L. On the other hand, NRAPOP-S (Figure 4B) followed a similar trend to that of NRAPOP-O but the adsorption capacity and the reducing efficiency was lower by10–15%. This difference in the efficiencies can be attributed to the magnitude of the positive charge density on the two polymers at this pH, as indicated above. These results indicate that as the dosage increases, more sites on the polymers become available for adsorption and reduction of Cr(VI).
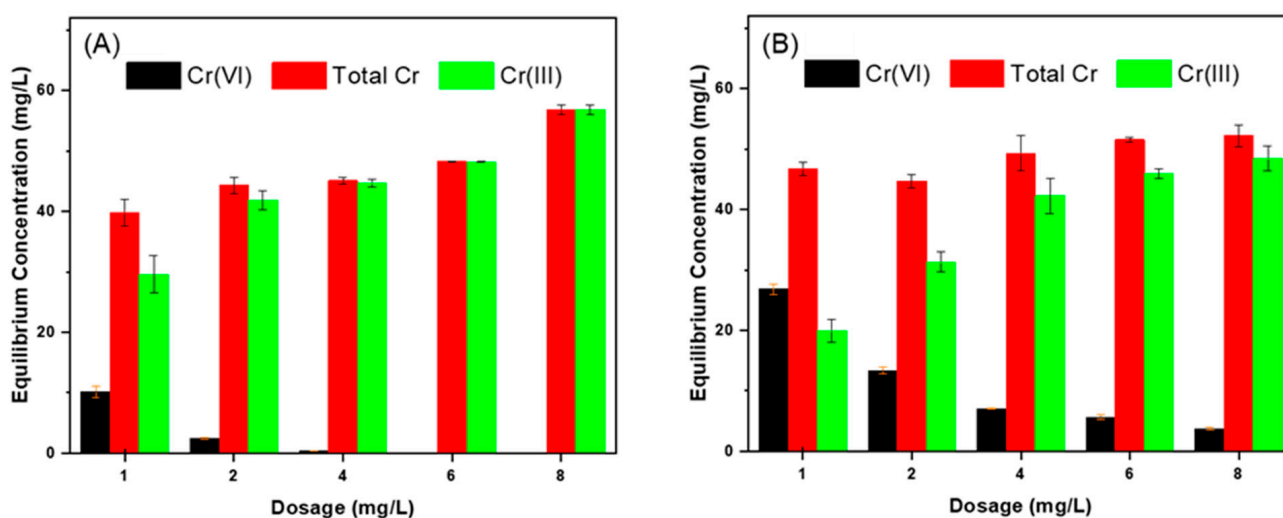
Figure 4. Effect of dosage on the adsorption and reduction of Cr(VI) using NRAPOP-O (**A**) and NRAPOP-S (**B**). Experimental conditions: pH: 2, contact time: 4 days, stirring speed: 175 rpm, temperature: 25 °C, sample volume: 5 mL, initial Cr(VI) concentration: 100 mg/L.

3.3.3. Effect of Contact Time

In order to better understand the kinetics and economic feasibility of the adsorption–reduction process of Cr(VI) by NRAPOPs, we investigated the effect of contact time between the two polymers and the chromate solution on the efficiency of the Cr(VI) removal and reduction. The changes in the concentration of Cr(VI), Cr(III), and total Cr in the solution were monitored over a period of twelve days upon the incubation of NRAPOPs at a dosage of 4 g/L with chromate solution at 100 mg/L and pH of 2. The results show that most (>95%) Cr(VI) was adsorbed by NRAPOP-O within three days and completely removed after six days (Figure 5A). On the other hand, the removal of Cr(VI) by NRAPOP-S showed slower progress with high slope for the first three days, leveling off between three and six days, followed by slower slope after six days, with complete removal after twelve days (Figure 5B). Inspection of this figure reveals that a simultaneous opposing trend was observed for the behavior of the concentrations of Cr(III) and total Cr.
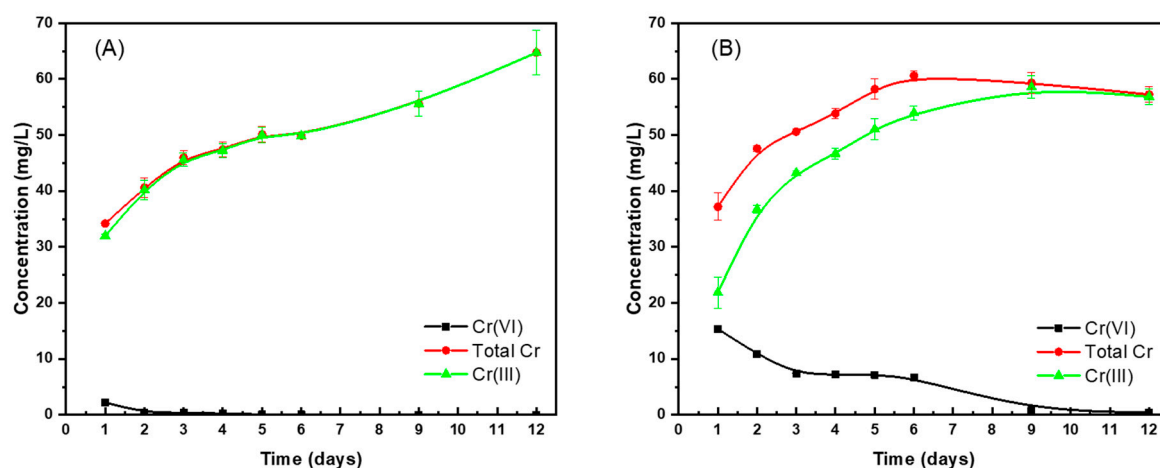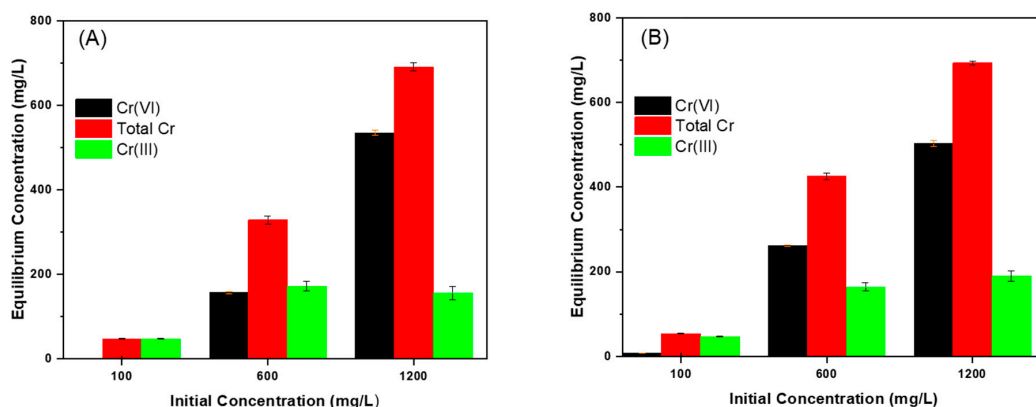
Figure 5. Effect of contact time on the adsorption and reduction of Cr(VI) using NRAPOP-O (**A**) and NRAPOP-S (**B**). Experimental conditions: pH: 2, dosage: 4 g/L, stirring speed: 175 rpm, temperature: 25 °C, sample volume: 5 mL, initial Cr(VI) concentration: 100 mg/L.

In order to explain the observed kinetic behavior, the following mechanism is proposed based on similar studies in the literature [39,58]. The process can be divided into three steps; the first is the adsorption on the surface with the possibility of diffusion to inner sites through the micropores of the polymers, followed by the second step which involves the reduction of Cr(VI) to Cr(III), and then followed by the third step which involved the release of Cr((III) into solution. The kinetic behavior of NRAPOP-O indicates that all the above involved steps are relatively fast as compared to NRAPOP-S with efficient desorption of Cr(III). These results are consistent with our previous explanation that the charge density plays a major role in the affinity of the two polymers towards Cr(VI) uptake, thus explaining the difference in the first step.

3.3.4. Effect of Initial Concentration

The equilibrium concentration of Cr(VI) was monitored as function of its initial concentration ranging from 100 mg/L to 1200 mg/L, while the dosage of the NRAPOPs was fixed at 4 g/L (Figure 6). The results show that as the initial concentration of the metal increases, the amount of Cr(VI) and total chromium in solution increases. The concentration of Cr(III) released into solution showed almost same value of the initial concentration of Cr(VI) at 100 mg/L, then it remained almost constant at higher initial concentration. In percentages, inspection of Figure 6 reveals that [Cr(VI)] remaining in solution increased from <1% to 44.6% of the initial concentration as it increased from 100 mg/L to 1200 mg/L. This was accompanied by a simultaneous decrease in [Cr(III)] from 99% to 22.5% of the initial chromium concentration in solution. At this stage, the loading capacity on the polymer was calculated by measuring the mass of Cr(VI) adsorbed in mg divided by the mass of the polymers in g. We attribute this decrease in the percentage of Cr(III) to the increase in the loading capacity of the polymers from 13.2 mg/g at the initial concentration of 100 mg/L to 127.4 mg/g at 1200 mg/L. As more Cr(VI) is loaded into the matrix of the polymers, the number of available active sites in the polymers decreases. This could explain the increase in the equilibrium [Cr(VI)] in solution as a result of limited available sites on the polymers. As indicated previously, the reduction and the desorption steps are much slower than the adsorption step, hence these steps are considered to be the rate determining steps which dictate the concentration of the desorbed Cr(III) into solution, leading to the observed constant value after four days of contact time (Figure 6). It is worth noting that neither adsorption isotherms, thermodynamic analysis, nor kinetic models could be applied in these cases due to the complex nature of the mechanism involved.
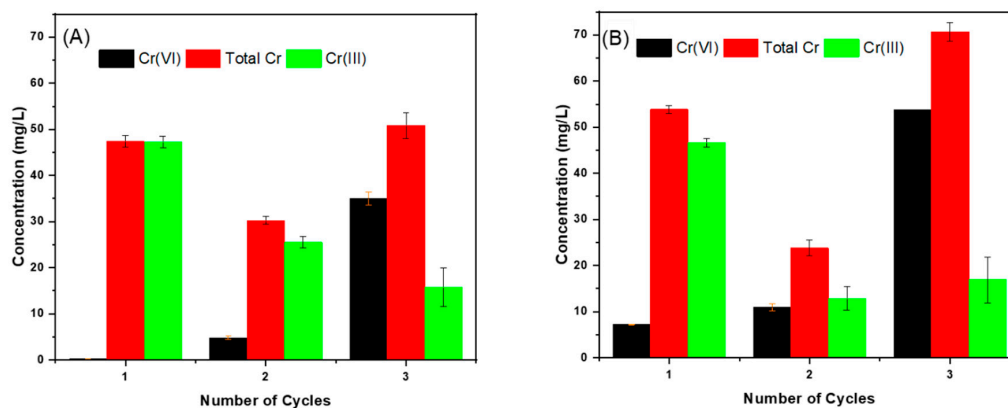
Figure 6. Effect of initial Cr(VI) concentration on the adsorption and reduction of Cr(VI) using NRAPOP-O (**A**) and NRAPOP-S (**B**). Experimental conditions: pH: 2, dosage: 4 g/L, stirring speed: 175 rpm, temperature: 25 °C, sample volume: 5 mL, time: 4 days.
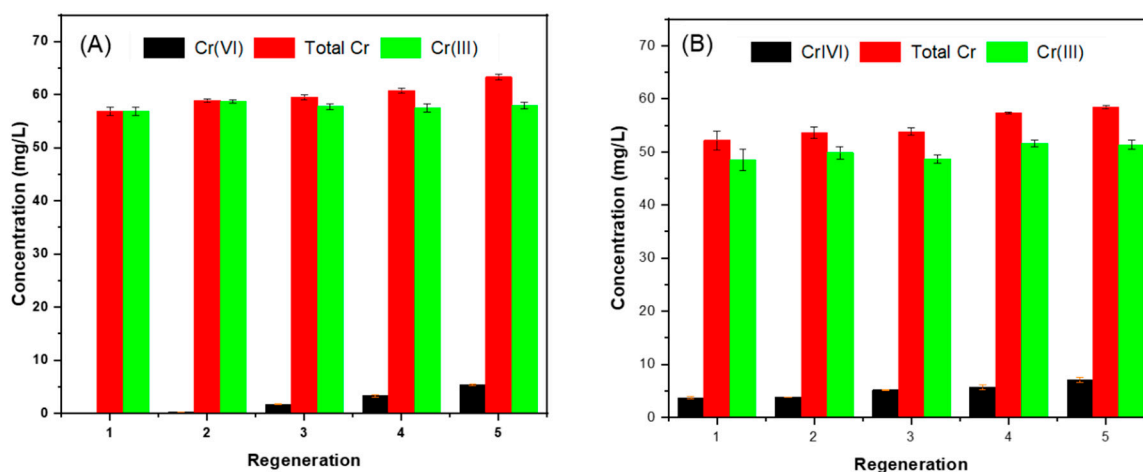
3.4. Reuse and Regeneration of NRAPOPs

The removal efficiency of Cr(VI) by the two NRAPOPs was also tested over three consecutive adsorption cycles from fresh Cr(VI)-contaminated solutions. The polymers were incubated with Cr(VI) solution at 100 mg/L for four days before the NRAPOPs were filtered; the process was then repeated twice with fresh solutions of chromate solutions. The concentrations of the Cr(VI), Cr(III) and total Cr were measured for these three solutions (Figure 7). Results show that for both polymers the amount of Cr(VI) removed from the solution and the amount of Cr(III) released into the solution continuously decreased for the second and third cycles. For NRAPOP-O, hardly any Cr(VI) remained in the first cycle, but for the second and third cycle, the concentrations of Cr(VI) were 5.0 and 35 mg/L, respectively (Figure 7A). Meanwhile, the concentration of Cr(III) in solution decreased from ~47.2 mg/L in first cycle to 25.0 and 15.8 mg/L for the second and third cycles, respectively. Similar trends were observed for NRAPOP-S (Figure 7B) but with Cr(VI) concentration starting at ~7.2 mg/L and increasing to ~53.8 mg/L and that of Cr(III) starting about ~46.7 mg/L and decreasing to ~16.9 mg/L between first and third cycles. These observations indicate that the efficiencies of the uptake of Cr(VI) and its subsequent reduction and release into solution decrease with number of cycles. Such a decrease could be attributed to two factors: (1) depletion of adsorption active sites due to their occupancy by Cr(VI) that remained in the polymer after 4 days and (2) diminution of the oxidation active sites due to the reduction of Cr(VI) to Cr(III).

Figure 7. Effect of number of cycles on removal of Cr(VI) and its reduction to Cr(III) by NRAPOP-O (**A**) and NRAPOP-S (**B**). Experimental conditions: pH: 2, dosage: 4 g/L, stirring speed: 175 rpm, temperature: 25 °C, sample volume: 5 mL, time: 4 days, initial concentration: 100 mg/L for each run.

In order to maintain a high adsorption and reduction efficiency of Cr(VI) by NRAPOPs over multiple cycles of use, we investigated the effect of the reducing agent hydrazine hydrate on the performance of polymers as a function of the number of cycles [29]. Thus, after NRAPOPs were incubated with Cr(VI) solutions at 100 mg/L, the polymers were filtered and incubated with hydrazine hydrate (10 mM) for four hours. This reducing agent regenerates the reducing sites of the NRAPOPs and causes the reduction of any Cr(VI) that is still trapped in the polymer, which is then released it to the solution. The POPs were then filtered and washed and incubated with fresh solution of Cr(VI) at 100 mg/L. This was repeated for five cycles and the concentrations of Cr(VI) and total Cr were measured after every adsorption process. The results exhibited in Figure 8 show that the polymers were able to remove Cr(VI) from solution over five cycles of regeneration with insignificant decrease (<5%) in the efficiency of removal. Such results indicate that the adsorption and reduction efficiency of the NRAPOPs can be fully regenerated (Figure S3) by the use of strong reducing agents such as hydrazine hydrate and suggest that the NRAPOPs have the potential for application in continuous-flow adsorption setups for the cleaning of Cr(VI)-contaminated water.

Figure 8. Regeneration and reuse of Cr(VI) sample multiple times on the adsorption and reduction of Cr(VI) using NRAPOP-O (**A**) and NRAPOP-S (**B**). Experimental conditions: pH: 2, dosage: 8 g/L, stirring speed: 175 rpm, temperature: 25 °C, sample volume: 5 mL, time: 4 days, initial concentration: 100 mg/L for each run.

4. Conclusions

We have synthesized two novel nitrogen-rich aminal-linked porous organic polymers, NRAPOP-O and NRAPOP-S, using a one-step Schiff base process. The two polymers were found to be thermally stable up to 400 °C, amorphous, and highly porous with surface areas of 692 and 803 m^2g^{-1}, respectively. Both NRAPOPs were able to remove Cr(VI) from solution and simultaneously reduce it to Cr(III), which was then released into the solution. At a polymer dosage of 4 g/L and pH = 2, the NRAPOPs were able to remove and reduce more than 99% of the 100 ppm Cr(VI) initial concentration. However, it was found that the adsorption and reduction efficiency of NRAPOP-O is higher than that of NRAPOP-S. The relative concentration of Cr(VI) that was removed and reduced decreased when the polymers were reused for subsequent cycles of the same concentration (100 ppm) of Cr(VI) or as its initial concentration increased. On the other hand, the NRAPOPs' adsorption and reduction activities were fully recovered upon treatment with hydrazine hydrate over five cycles of adsorption and regeneration. Therefore, the NRAPOPs can be considered promising adsorbents for removal of Cr(VI) from contaminated streams of wastewater and its conversion to the beneficial ion Cr(III). Competitive adsorption and the effect of other organic and inorganic pollutants on the efficiency of removal of Cr(VI) and protection of NRAPOPs will be the subject of a new study in our group. In addition, we plan to utilize pollutants that can be adsorbed by the NRAPOPs and can be more easily oxidized than the

NRAPOPs such that the oxidation by-products are released into solution, thus freeing and preserving the adsorption sites on the adsorbent for further utilization.

References

1. Malaviya, P.; Singh, A. Physicochemical technologies for remediation of chromium-containing waters and wastewaters. *Crit. Rev. Environ. Sci. Technol.* **2011**, *41*, 1111–1172. [CrossRef]
2. Khezami, L.; Capart, R. Removal of chromium(VI) from aqueous solution by activated carbons: Kinetic and equilibrium studies. *J. Hazard. Mater.* **2005**, *123*, 223–231. [CrossRef] [PubMed]
3. Gode, F.; Pehlivan, E. Sorption of Cr(III) onto chelating b-DAEG-sporopollenin and CEP-sporopollenin resins. *Bioresour. Technol.* **2007**, *98*, 904–911. [CrossRef] [PubMed]
4. Costa, M. Potential hazards of hexavalent chromate in our drinking water. *Toxicol. Appl. Pharmacol.* **2003**, *188*, 1–5. [CrossRef]
5. Kotaś, J.; Stasicka, Z. Chromium occurrence in the environment and methods of its speciation. *Environ. Pollut.* **2000**, *107*, 263–283. [CrossRef]
6. Dakiky, M.; Khamis, M.; Manassra, A.; Mer'eb, M. Selective adsorption of chromium(VI) in industrial wastewater using low-cost abundantly available adsorbents. *Adv. Environ. Res.* **2002**, *6*, 533–540. [CrossRef]
7. McNeill, L.S.; McLean, J.E.; Parks, J.L.; Edwards, M.A. Hexavalent chromium review, part 2: Chemistry, occurrence, and treatment. *J. Am. Water Works Assoc.* **2012**, *104*, E395–E405. [CrossRef]
8. McLean, J.E.; McNeill, L.S.; Edwards, M.A.; Parks, J.L. Hexavalent chromium review, part 1: Health effects, regulations, and analysis. *J. Am. Water Works Assoc.* **2012**, *104*, E348–E357. [CrossRef]
9. Wilbur, S.; Abadin, H.; Fay, M.; Yu, D.; Tencza, B.; Ingerman, L.; Klotzbach, J.; James, S. *Toxicological Profile for Chromium*; Agency for Toxic Substances and Disease Registry: Atlanta, GA, USA, 2012.
10. Owlad, M.; Aroua, M.K.; Daud, W.A.W.; Baroutian, S. Removal of hexavalent chromium-contaminated water and wastewater: A review. *Water Air Soil Pollut.* **2009**, *200*, 59–77. [CrossRef]
11. Zhu, J.; Wei, S.; Gu, H.; Rapole, S.B.; Wang, Q.; Luo, Z.; Haldolaarachchige, N.; Young, D.P.; Guo, Z. One-pot synthesis of magnetic graphene nanocomposites decorated with core@double-shell nanoparticles for fast chromium removal. *Environ. Sci. Technol.* **2012**, *46*, 977–985. [CrossRef]
12. Orozco, A.M.F.; Contreras, E.M.; Zaritzky, N.E. Cr(VI) reduction capacity of activated sludge as affected by nitrogen and carbon sources, microbial acclimation and cell multiplication. *J. Hazard. Mater.* **2010**, *176*, 657–665. [CrossRef] [PubMed]
13. Qiu, B.; Wang, Y.; Sun, D.; Wang, Q.; Zhang, X.; Weeks, B.L.; O'Connor, R.; Huang, X.; Wei, S.; Guo, Z. Cr(VI) removal by magnetic carbon nanocomposites derived from cellulose at different carbonization temperatures. *J. Mater. Chem. A* **2015**, *3*, 9817–9825. [CrossRef]
14. Yu, Z.; Zhang, X.; Huang, Y. Magnetic chitosan-iron(III) hydrogel as a fast and reusable adsorbent for chromium(VI) removal. *Ind. Eng. Chem. Res.* **2013**, *52*, 11956–11966. [CrossRef]
15. Krishna Kumar, A.S.; Jiang, S.J.; Tseng, W.L. Effective adsorption of chromium(VI)/Cr(III) from aqueous solution using ionic liquid functionalized multiwalled carbon nanotubes as a super sorbent. *J. Mater. Chem. A* **2015**, *3*, 7044–7057. [CrossRef]
16. Mohan, D.; Pittman, C.U. Activated carbons and low cost adsorbents for remediation of tri- and hexavalent chromium from water. *J. Hazard. Mater.* **2006**, *137*, 762–811. [CrossRef] [PubMed]
17. Zhou, X.; Korenaga, T.; Takahashi, T.; Moriwake, T.; Shinoda, S. A process monitoring/controlling system for the treatment of wastewater containing chromium(VI). *Water Res.* **1993**, *27*, 1049–1054. [CrossRef]

18. Tiravanti, G.; Petruzzelli, D.; Passino, R. Pretreatment of tannery wastewaters by an ion exchange process for Cr(III) removal and recovery. *Water Sci. Technol.* **1997**, *36*, 197–207. [CrossRef]

19. Khamis, M.; Jumean, F.; Abdo, N. Speciation and removal of chromium from aqueous solution by white, yellow and red UAE sand. *J. Hazard. Mater.* **2009**, *169*, 948–952. [CrossRef]

20. Dahbi, S.; Azzi, M.; De La Guardia, M. Removal of hexavalent chromium from wastewaters by bone charcoal. *Fresenius J. Anal. Chem.* **1999**, *363*, 404–407. [CrossRef]

21. Kongsricharoern, N.; Polprasert, C. Chromium removal by a bipolar electro-chemical precipitation process. *Water Sci. Technol.* **1996**, *34*, 109–116. [CrossRef]

22. Pagilla, K.R.; Canter, L.W. Laboratory studies on remediation of chromium-contaminated soils. *J. Environ. Eng.* **1999**, *125*, 243–248. [CrossRef]

23. Almeida, J.C.; Cardoso, C.E.D.; Tavares, D.S.; Freitas, R.; Trindade, T.; Vale, C.; Pereira, E. Chromium removal from contaminated waters using nanomaterials—A review. *TrAC Trends Anal. Chem.* **2019**, *118*, 277–291. [CrossRef]

24. GracePavithra, K.; Jaikumar, V.; Kumar, P.S.; SundarRajan, P.S. A review on cleaner strategies for chromium industrial wastewater: Present research and future perspective. *J. Clean. Prod.* **2019**, *228*, 580–593. [CrossRef]

25. Kim, W.; Park, J.Y.; Kim, Y. Fabrication of branched-TiO_2 microrods on the FTO glass for photocatalytic reduction of Cr(VI) under visible-light irradiation. *J. Ind. Eng. Chem.* **2019**, *73*, 248–253. [CrossRef]

26. Jiang, B.; Gong, Y.; Gao, J.; Sun, T.; Liu, Y.; Oturan, N.; Oturan, M.A. The reduction of Cr(VI) to Cr(III) mediated by environmentally relevant carboxylic acids: State-of-the-art and perspectives. *J. Hazard. Mater.* **2019**, *365*, 205–226. [CrossRef]

27. Qian, A.; Liao, P.; Yuan, S.; Luo, M. Efficient reduction of Cr(VI) in groundwater by a hybrid electro-Pd process. *Water Res.* **2014**, *48*, 326–334. [CrossRef]

28. Wani, P.A.; Wahid, S.; Khan, M.S.A.; Rafi, N.; Wahid, N. Investigation of the role of chromium reductase for Cr(VI) reduction by *Pseudomonas* species isolated from Cr(VI) contaminated effluent. *Biotechnol. Res. Innov.* **2019**, *3*, 38–46. [CrossRef]

29. Ding, J.; Pu, L.; Wang, Y.; Wu, B.; Yu, A.; Zhang, X.; Pan, B.; Zhang, Q.; Gao, G. Adsorption and Reduction of Cr(VI) together with Cr(III) sequestration by polyaniline confined in pores of polystyrene beads. *Environ. Sci. Technol.* **2018**, *52*, 12602–12611. [CrossRef]

30. Lu, Y.Z.; Fu, L.; Ding, J.; Ding, Z.W.; Li, N.; Zeng, R.J. Cr(VI) reduction coupled with anaerobic oxidation of methane in a laboratory reactor. *Water Res.* **2016**, *102*, 445–452. [CrossRef]

31. Wang, L.; Wang, N.; Zhu, L.; Yu, H.; Tang, H. Photocatalytic reduction of Cr(VI) over different TiO_2 photocatalysts and the effects of dissolved organic species. *J. Hazard. Mater.* **2008**, *152*, 93–99. [CrossRef]

32. Pan, X.; Liu, Z.; Chen, Z.; Cheng, Y.; Pan, D.; Shao, J.; Lin, Z.; Guan, X. Investigation of Cr(VI) reduction and Cr(III) immobilization mechanism by planktonic cells and biofilms of *Bacillus subtilis* ATCC-6633. *Water Res.* **2014**, *55*, 21–29. [CrossRef] [PubMed]

33. Pakade, V.E.; Tavengwa, N.T.; Madikizela, L.M. Recent advances in hexavalent chromium removal from aqueous solutions by adsorptive methods. *RSC Adv.* **2019**, *9*, 26142–26164. [CrossRef]

34. Xie, A.; Ji, L.; Luo, S.; Wang, Z.; Xu, Y.; Kong, Y. Synthesis, characterization of poly(m-phenylenediamine)/palygorskite and its unusual and reactive adsorbability to chromium(VI). *New J. Chem.* **2014**, *38*, 777–783. [CrossRef]

35. Saha, B.; Orvig, C. Biosorbents for hexavalent chromium elimination from industrial and municipal effluents. *Coord. Chem. Rev.* **2010**, *254*, 2959–2972. [CrossRef]

36. Solgi, M.; Najib, T.; Ahmadnejad, S.; Nasernejad, B. Synthesis and characterization of novel activated carbon from Medlar seed for chromium removal: Experimental analysis and modeling with artificial neural network and support vector regression. *Resour. Technol.* **2017**, *3*, 236–248. [CrossRef]

37. Kan, C.C.; Ibe, A.H.; Rivera, K.K.P.; Arazo, R.O.; de Luna, M.D.G. Hexavalent chromium removal from aqueous solution by adsorbents synthesized from groundwater treatment residuals. *Sustain. Environ. Res.* **2017**, *27*, 163–171. [CrossRef]

38. Ray, P.; Sabri, M.A.; Ibrahim, T.H.; Khamis, M.I.; Jumean, F.H. Design and optimization of a batch sequential contactor for the removal of chromium(VI) from industrial wastewater using sheep wool as a low-cost adsorbent. *Desalin. Water Treat.* **2018**, *113*, 109–113. [CrossRef]

39. Jumean, F.H.; Khamis, M.I.; Sara, Z.A.; AbouRich, M.S. Concurrent removal and reduction of Cr(VI) by wool: Short and long term equilibration studies. *Am. J. Anal. Chem.* **2015**, *6*, 47–57. [CrossRef]

40. Das, S.; Heasman, P.; Ben, T.; Qiu, S. Porous organic materials: Strategic design and structure-function correlation. *Chem. Rev.* **2017**, *117*, 1515–1563. [CrossRef]

41. Zhang, T.; Xing, G.; Chen, W.; Chen, L. Porous organic polymers: A promising platform for efficient photocatalysis. *Mater. Chem. Front.* **2020**, *4*, 332–353. [CrossRef]

42. Enjamuri, N.; Sarkar, S.; Reddy, B.M.; Mondal, J. Design and catalytic application of functional porous organic polymers: Opportunities and challenges. *Chem. Rec.* **2019**, *19*, 1782–1792. [CrossRef] [PubMed]

43. Arab, P.; El-Kadri, O.M.; El-Kaderi, H.M. Designing functional porous organic frameworks for gas storage and separation. In *Monographs in Supramolecular Chemistry*; RSC Publishing: Cambridge, UK, 2017; pp. 388–411. ISBN 9781782624172.

44. Kassab, R.M.; Jackson, K.T.; El-Kadri, O.M.; El-Kaderi, H.M. Nickel-catalyzed synthesis of nanoporous organic frameworks and their potential use in gas storage applications. *Res. Chem. Intermed.* **2011**, *37*, 747–757. [CrossRef]

45. Rabbani, M.G.; Sekizkardes, A.K.; El-Kadri, O.M.; Kaafarani, B.R.; El-Kaderi, H.M. Pyrene-directed growth of nanoporous benzimidazole-linked nanofibers and their application to selective CO_2 capture and separation. *J. Mater. Chem.* **2012**, *22*, 25409–25417. [CrossRef]

46. El-Kadri, O.M.; Tessema, T.D.; Almotawa, R.M.; Arvapally, R.K.; Al-Sayah, M.H.; Omary, M.A.; El-Kaderi, H.M. Pyrene bearing azo-functionalized porous nanofibers for CO_2 separation and toxic metal cation sensing. *ACS Omega* **2018**, *3*, 15510–15518. [CrossRef] [PubMed]

47. Cui, F.; Liang, R.; Qi, Q.; Jiang, G.; Zhao, X. Efficient Removal of Cr(VI) from aqueous solutions by a dual-pore covalent organic framework. *Adv. Sustain. Syst.* **2019**, *3*, 1800150. [CrossRef]

48. Zhu, D.; Zhou, S.; Zhou, Z.; Li, R.; Ye, J.; Ziyu, X.; Lan, S.; Zhang, Y.; Miao, S.; Wang, W. Highly efficient and selective removal of Cr(VI) by covalent organic frameworks: Structure, performance and mechanism. *Colloids Surfaces A Physicochem. Eng. Asp.* **2020**, *600*. [CrossRef]

49. Chen, J.; Wang, Y.; Ye, C.; Lyu, W.; Zhu, J.; Yan, W.; Qiu, T. Self-reducible conjugated microporous polyaniline for long-term selective Cr(VI) detoxication driven by tunable pore dimension. *ACS Appl. Mater. Interfaces* **2020**, *12*, 28681–28691. [CrossRef]

50. Sen, S.; Al-Sayah, M.H.; Mohammed, M.S.; Abu-Abdoun, I.I.; El-Kadri, O.M. Multifunctional nitrogen-rich aminal-linked luminescent porous organic polymers for iodine enrichment and selective detection of Fe^{3+} ions. *J. Mater. Sci.* **2020**, *55*, 10896–10909. [CrossRef]

51. Abdelmoaty, Y.H.; Tessema, T.D.; Choudhury, F.A.; El-Kadri, O.M.; El-Kaderi, H.M. Nitrogen-rich porous polymers for carbon dioxide and iodine sequestration for environmental remediation. *ACS Appl. Mater. Interfaces* **2018**, *10*, 16049–16058. [CrossRef]

52. Sabri, M.A.; Al-Sayah, M.H.; Sen, S.; Ibrahim, T.H.; El-Kadri, O.M. Fluorescent aminal linked porous organic polymer for reversible iodine capture and sensing. *Sci. Rep.* **2020**, *10*, 15943. [CrossRef]

53. Cañas-Ventura, M.E.; Xiao, W.; Wasserfallen, D.; Müllen, K.; Brune, H.; Barth, J.V.; Fasel, R. Self-assembly of periodic bicomponent wires and ribbons. *Angewandte Chemie Int. Ed.* **2007**, *46*, 1814–1818. [CrossRef] [PubMed]

54. Song, W.C.; Xu, X.K.; Chen, Q.; Zhuang, Z.Z.; Bu, X.H. Nitrogen-rich diaminotriazine-based porous organic polymers for small gas storage and selective uptake. *Polym. Chem.* **2013**, *4*, 4690–4696. [CrossRef]

55. Schwab, M.G.; Fassbender, B.; Spiess, H.W.; Thomas, A.; Feng, X.; Müllen, K. Catalyst-free preparation of melamine-based microporous polymer networks through Schiff base chemistry. *J. Am. Chem. Soc.* **2009**, *131*, 7216–7217. [CrossRef] [PubMed]

56. Weng, J.Y.; Xu, Y.L.; Song, W.C.; Zhang, Y.H. Tuning the adsorption and fluorescence properties of aminal-linked porous organic polymers through N-heterocyclic group decoration. *J. Polym. Sci. Part A Polym. Chem.* **2016**, *54*, 1724–1730. [CrossRef]

57. Pan, X.; Qin, X.; Zhang, Q.; Ge, Y.; Ke, H.; Cheng, G. N- and S-rich covalent organic framework for highly efficient removal of indigo carmine and reversible iodine capture. *Microporous Mesoporous Mater.* **2020**, *296*, 109990. [CrossRef]

58. Odeh, L.; Odeh, I.; Khamis, M.; Khatib, M.; Qurie, M.; Shakhsher, Z.; Qutob, M. Hexavalent chromium removal and reduction to Cr(III) by polystyrene tris(2-aminoethyl)amine. *Am. J. Anal. Chem.* **2015**, *6*, 26–37. [CrossRef]